



TITLE:

Topics on High Energy Spin Physics : Nucleon Polarization and Multi-Quark Resonances : To Prof. Takuji Yanabu, who has shown us the way of studying physics for more than 20 years. (Commemoration Issue Dedicated to Professor Takuji Yanabu on the Occasion of his Retirement)

AUTHOR(S):

Masaïke, Akira

---

CITATION:

Masaïke, Akira. Topics on High Energy Spin Physics : Nucleon Polarization and Multi-Quark Resonances : To Prof. Takuji Yanabu, who has shown us the way of studying physics for more than 20 years. (Commemoration Issue Dedicated to Professor Takuji Yanabu on the Occasion of his Retirement). Bulletin of the Institute for Chemical Research, Kyoto U...

ISSUE DATE:

1982-08-31

URL:

<http://hdl.handle.net/2433/76970>

RIGHT:

REVIEW

## Topics on High Energy Spin Physics

### —Nucleon Polarization and Multi-Quark Resonances—

—To Prof. Takuji Yanabu, who has shown us the way of  
studying physics for more than 20 years.

Akira MASAIKE

*Received March 31, 1982*

New methods to get pure spin states of nuclei are described. They are important tools for high energy spin physics. Especially recent developments of the polarized target and the polarized beam are explained. Some results of polarization experiments for the search of multi-quark resonances as dibaryons and  $Z^*$  are also shown. The greater part of this report is the experimental works performed in KEK.

KEY WORDS: High energy spin physics/ Polarized target and beam/ Nucleon polarization/ Multi-quark resonances/

### I. INTRODUCTION

From the past lessons on spin dependent phenomena in the high energy physics and the nuclear physics, we believe that the "spin" must be one of the most important tools for the research on the fundamental interaction of the elementary particles. We remember that the parity non-conservation of the weak interaction was found by the measurement of the asymmetry of the  $\beta$ -decay from polarized  $^{60}\text{Co}$  nuclei. We know another example, that is, the shell structure of the nuclei was established by the introduction of the spin-orbit interaction of nucleons in the nucleus. The spin experiments gave us sometimes unexpected new phenomena, which disturbed our conventional picture of nuclear and sub-nuclear matter. Furthermore most of the models of nuclear and high energy interactions have been baptized with spin dependent experiments.

Recently it was pointed out that the measurement of spin dependent parameters of hadron-hadron scattering plays important role in studying the mechanism of the high energy interaction. Especially for search of the multi-quark systems, experiments on the spin are indispensable. Perhaps the spin is becoming one of the frontier research areas along with high energy physics.

For these experiments we have to have pure spin states of nuclei, which requires polarized beams and polarized targets and sometimes polarization analysis of scattered particles.

In this review article, we should like to describe the developments of new methods to get the pure spin states of nuclei and the recent results of polarization experiments for the search of multi-quark resonances, which is one of the topics on the high energy spin physics. The greater part of this article is the experimental works performed in KEK.

政池 明: KEK, National Laboratory for High Energy Physics, Oho-machi, Tsukuba, Ibaraki.

## II. TOOLS FOR HIGH ENERGY SPIN PHYSICS

### i) Recent Development of Polarized Target

It is well known that an assembly of nuclei of magnetic moments in matter in thermal equilibrium at a temperature  $T$  and a magnetic field  $H$  orient themselves in the direction of the field. The orientation is not perfect because of the thermal energy  $kT$ . The degree of nuclear polarization  $P_n$  is the ensemble average  $\langle I_z \rangle / I$ , taken over all the spins of the nuclei in the sample. For a spin  $I=1/2$ ,  $P_n$  is given by:

$$P_n = \tanh\left(\frac{\mu H}{kT}\right) \quad (2-1)$$

In the case of protons it is

$$P_n = \tanh\left(1.02 \times 10^{-7} \frac{H}{T}\right) \quad (2-2)$$

It is desirable to get quite high polarization of nucleus for the high energy spin physics. In order to obtain high polarization of nucleus, we have to have quite low temperature and high magnetic field. Dilution refrigerators and high field superconducting coils may open in the future a way for such a high polarization. Such a method of polarization is the so-called "brute force" method.

On the other hand, we can get sizable polarization of the nuclei in paramagnetic material by dynamical methods in rather lower field and higher temperature than in the case of brute force method.<sup>1)</sup> Dynamical methods use the magnetic couplings between electronic and nuclear spins to transfer the polarization of electrons to the nucleus. These methods originally proposed by Overhauser<sup>2)</sup> who predicted that in metals the saturation of the spin resonance of conduction electrons could lead to a nuclear polarization comparable to the electronic polarization but of opposite sign. Shortly afterward the prediction was confirmed by an experiment and then it was shown by A. Abragam that the similar method could be extended to non-metallic substances and in particular to liquids and solids containing in solution paramagnetic impurities, which is important for the polarized target.<sup>3)</sup> He also showed that the paramagnetic center and the nucleus being polarized need not belong to the same atom and that the coupling between the center and the nucleus is magnetic dipole-dipole interaction which provides the partially forbidden mutual-spin flip transitions. This phenomenon was named "solid effect", which made it possible to consider the polarization of any nucleus by dynamic method. The solid effect has proved the most useful method for obtaining the high proton polarization.

Figure 2-1 illustrates the energy level diagram of a paramagnetic center coupled to a single neighboring proton in external magnetic field. In this figure  $m_e$  and  $m_p$  are the spin projection eigenvalues of the paramagnetic center and the proton. The splitting by the electron Zeeman interaction is larger than that by the proton Zeeman interaction by factor 600. Transitions  $a$  and  $b$  in Fig. 2-1 are the "forbidden" transitions in which both  $m_e$  and  $m_p$  reverse the sign. On the other hand, transitions  $a'$  and  $b'$  in Fig. 2-1 in which  $m_e$  reverses and  $m_p$  remains the same are called the "allowed transition". The transition probability for the "forbidden transition" is much smaller than that for the

## Spin Physics in High Energy

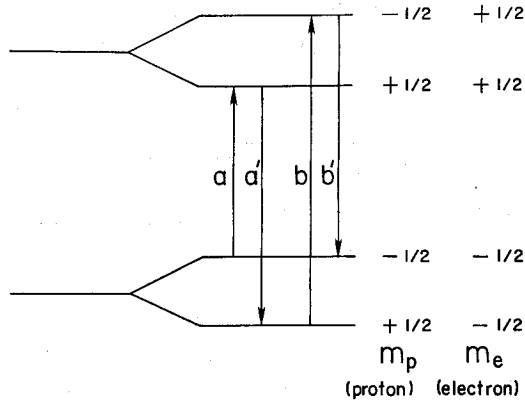


Fig. 2-1 Energy level diagram of paramagnetic center coupled to a single neighboring proton in a external magnetic field.

“allowed transition”. However the dipole-dipole coupling does ensure that there is a small admixture of  $m_e = +1/2$  and  $-1/2$ . This admixture makes possible the forbidden transitions by the RF field which is applied at the frequency corresponds to the energy difference of the two levels. If sufficient power to saturate this transition is applied, the populations of the two levels connected by the forbidden transition can be equalized. It corresponds to the “flip-flop” of an electron spin and a proton spin in Fig. 2-2. Because of the strong coupling between the electron and the lattice, the relaxation time of the electron ( $T_{1e}$ ) is short. It corresponds to the allowed transition. Whereas, the proton spin stays on the level for long time, because of the weakness of the coupling between the proton spin and the lattice. Such processes clearly provide a means for the orientation of the proton spin.

As two neighbouring protons are coupled by dipole-dipole interaction, in which energy is conserved, the orientation of the proton spin diffuses throughout the whole sample, tending to equalize the nuclear polarization (Fig. 2-2).

At the beginning of the history of dynamically polarized proton target, crystal of

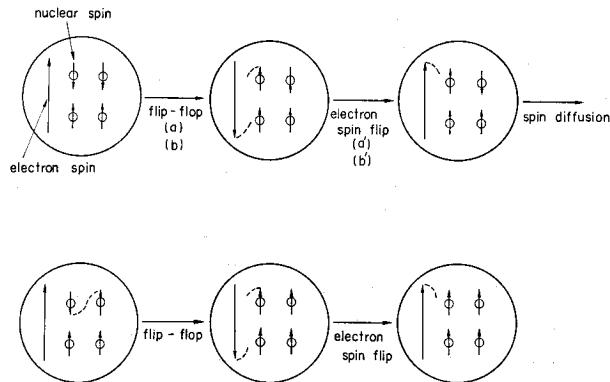


Fig. 2-2 Dynamic polarization of protons by the “flip-flop” of an electron spin and a proton spin. The spin diffusion is also illustrated.

lanthanum magnesium nitrate (LMN),  $\text{La}_2\text{Mg}_3(\text{NO}_3)_{12}\cdot 24\text{H}_2\text{O}$ , containing a small percentage (*e.g.* 0.2 %) of paramagnetic neodymium, was used. Nd ions act electron spins 1/2, with a *g*-factor having

$$g_{\parallel z} \simeq 0.4; \quad g_{\perp z} \simeq 2.70 \quad (2-3)$$

(*z* being a crystalline axis).

The proton polarization of about 70 % was produced in this sample in the field of 18 KG and at the temperature around 1°K.

The increasing interest in polarization phenomena in the high energy physics required target material having a larger free-to-bound nucleon ratio than LMN. After many trials of the development of target material, the high polarization of organic material with  $\text{Cr}^{\text{V}}$  complex in 0.5°K and 25 KG was discovered.<sup>4)</sup> In order to get lower temperature than 1°K,  $\text{He}^3$  cryostats of very high cooling power were constructed, which made it possible to obtain a high polarization in large target volume in a short time.

Recently dilution refrigerators with very high cooling power were constructed for the polarized target.<sup>5,6)</sup> The application of the dilution refrigerator to a polarized target is quite helpful in the measurement of the several spin dependent parameters of complicated reactions in the high energy physics. One of the advantages of the polarized target using dilution refrigerators is the long nuclear spin lattice relaxation time realized at quite low temperatures. The long relaxation time allows us to use the polarized target in a lower and less homogeneous field than the polarizing one. The method makes it easy to have a larger access angle for the incident and scattered particles. We can obtain higher polarization in a dilution refrigerator than in a  $\text{He}^3$  cryostat because of the lower temperature. It plays a remarkable role with the deuteron polarized target. The deuteron polarization of more than 40 % can be obtained by use of the dilution refrigerator. Furthermore high polarization of protons is very useful as a proton filter to polarize slow neutrons. For the polarized proton filter very high polarization must be kept quite stable for a long time. Such stability and high polarization of protons can be realized with a dilution refrigerator.

The principle of the dilution refrigerator is based on the phase separation of solutions of  $\text{He}^3$  and  $\text{He}^4$  below the critical temperature; the upper phase is richer than the lower phase in  $\text{He}^3$ . The lower part (dilute phase) is superfluid and  $\text{He}^4$  plays no significant thermodynamical or hydrodynamical role at very low temperature. Therefore,  $\text{He}^3$  of the dilute component in the lower part behaves like ideal gas. When  $\text{He}^3$  dilutes from the  $\text{He}^3$  rich phase to the dilute phase, it has a cooling power of

$$\dot{Q} \simeq \dot{n}(95T^2 - 12T_i^2) \quad (2-4)$$

where  $\dot{n}$  is the flow rate of  $\text{He}^3$  into the dilute phase in moles/sec,  $\dot{Q}$  is in watts and  $T$  is the temperature (°K) of a mixing chamber in which the phase separation occurs.  $T_i$  is the temperature (°K) of the incoming concentrated stream to the mixing chamber.  $\text{He}^3$  in the dilute phase is lead to a still through heat exchangers in which the incoming concentrated stream is cooled down by the outgoing dilute solution.  $\text{He}^3$  is pumped out from the still at a high rate at a temperature of 0.6°K~0.9°K, whereas the pumping rate of  $\text{He}^4$  is rather low because of lower vapor pressure of  $\text{He}^4$ . The principle is

## Spin Physics in High Energy

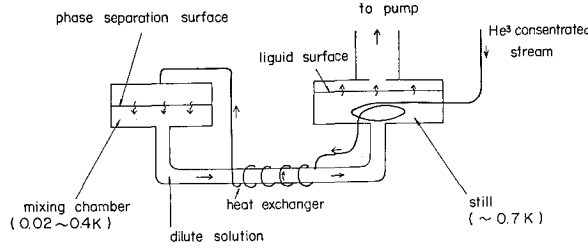


Fig. 2-3 Schematic view of the principle of the dilution refrigerator

shown schematically in Fig. 2-3. The dilution refrigerator was developed at KEK for a spin frozen proton and deuteron targets.<sup>5)</sup> It was designed to obtain very high cooling capacity over the wide temperature range, especially at the temperature of  $50\text{ m}^\circ\text{K} \sim 500\text{ m}^\circ\text{K}$ . It has a high gas flow rate (typically  $1 \times 10^{-2} \text{ mol} \cdot \text{s}^{-1}$ ), a powerful  $^4\text{He}$  precooling system and good heat exchange efficiency between the incoming stream and outgoing solution. It has double-tube heat exchangers, whose lower temperature parts are filled with sintered copper. Typical cooling power was about 90 mW at  $0.37^\circ\text{K}$  and 65 mW at  $0.33^\circ\text{K}$ . The proton polarization of about 98 % in propanediol and the deuteron polarization of about 40 % in deuterated propanediol (D-8) can be obtained with the dilution refrigerator in the magnetic field of 25 KG using the microwave of 70 GHz.

The polarizations of protons and deuterons can be measured by nuclear magnetic resonance (NMR). The proton NMR signal is observed at 106 MHz, which corresponds to a magnetic field of 25 KG. The area of the absorption signal is proportional to the proton polarization. The polarization is deduced by comparing the signal intensity in the dynamically polarized state with that in the thermal equilibrium state.<sup>7)</sup> Fig. 2-4(a) shows the NMR signal of the highly polarized proton ( $\sim 95\%$  polarization). The deuteron NMR frequency is 16.3 MHz in a 25 KG field. In the case of deuterons, the small magnetic moment and the inhomogeneous broadening of the signal due to quadrupole interaction make the deuteron NMR signal much smaller than the proton signal. According to the spin temperature hypothesis in the deuteron system, the polarization of the deuteron is calculated from the asymmetry of the polarized NMR signal.

$$P_D = \frac{R^2 - 1}{R^2 + R + 1} \quad (2-5)$$

where  $R$  is the ratio of the signal intensities corresponding to  $+1 \rightarrow 0$  and  $0 \rightarrow -1$  spin-state transitions. Fig. 2-4(b) shows the NMR signals of the polarized deuteron, in which one of two peaks corresponds to the transition between spin states of  $+1$  and  $0$  and the other corresponds to that between spin states of  $0$  and  $-1$ . The deuteron polarization can be determined by calculation of deuteron line-shape function with deuteron quadrupole coupling.<sup>8)</sup>

These polarized proton and deuteron targets opened a way for the precise studies of the high energy spin physics.

### ii) Polarized Beam for High Energy Physics

The possibility of accelerating polarized protons by a high energy synchrotron had

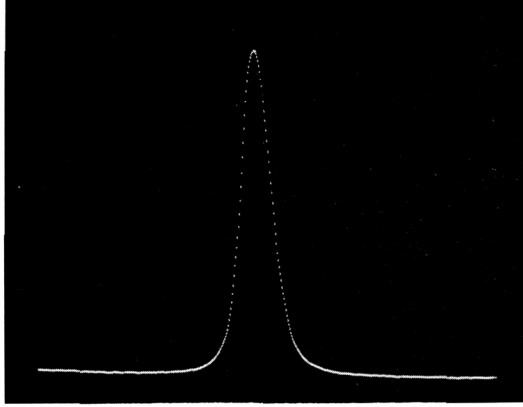
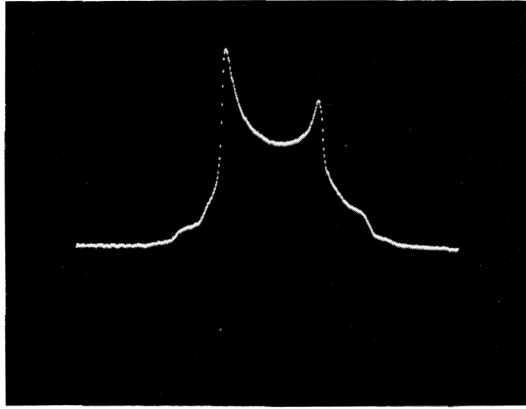


Fig. 2-4(a) NMR signal of highly polarized proton



(b) NMR signal of highly polarized deuteron

been considered for many years, and the realization of it was made in the ZGS, Argonne. The behavior of a polarized beam in a high energy synchrotron was studied by Froisart and Stora in 1960.<sup>9)</sup> Then the problem was also studied by many authors. Froisart and Stora concluded that there would be depolarization resonances, where the frequency of the Betatron oscillation is the same as the frequency of the Larmor precession of the proton spin. Such a resonance occurs at

$$\gamma G = n \pm \nu, \quad (2-6)$$

where  $\gamma$  is the relativistic factor,  $G$  the anomalous gyromagnetic ratio ( $G = g/2 - 1 = 1.7268$ ),  $\nu$  the vertical tune and  $n$  is an integer. The polarization after crossing the resonance is<sup>10)</sup>

$$\frac{P}{P_0} = 2 \exp\left(-\frac{\pi \varepsilon^2}{2\alpha}\right) - 1 \quad (2-7)$$

where  $\varepsilon$  is the resonance strength,  $\alpha$  is defined as

$$\alpha = (\dot{\gamma}G \mp \dot{\nu})/\omega_0, \quad (2-8)$$

$P_0$  is the polarization before crossing the resonance and  $\omega_0$  is the angular frequency of revolution. From these equations it can be shown that the spin flips if  $\pi\epsilon^2/2\alpha > 0.693$ . In this case the sign of the polarization reverses. This is due to an adiabatic passage through the resonance. On the other hand when the resonance is crossed rapidly at the proper  $\gamma$  value, there is very little loss of the polarization. Spin flip does not occur because the particles cross the resonance so rapidly and they stay on the resonance for quite a short time. It can be realized by changing the tune ( $\nu$ -jump), which can be obtained by pulsed quadrupole magnets.

There are also the imperfection resonances which occur at  $\gamma G = n$ . The resonance strengths of them can be estimated from the statistical expectation values of the harmonic amplitudes of vertical closed orbit distortion in the synchrotron.

As the ZGS synchrotron was a weak focusing accelerator, there were not so many resonances and they were not so strong as strong focusing machines. Actually in the case of ZGS there were 6 resonances up to 12 GeV, in which the beam was depolarized completely. In order to avoid the depolarization, 2 quadrupole magnets and a bending magnet were used, with which the beam passed through the resonances very rapidly. As ZGS synchrotron was closed in 1979, there has been no high energy polarized proton beam. There are plans to accelerate polarized beam in KEK and AGS. Both of them are strong focusing machines. Beam has to pass through 11 intrinsic resonances and 22 imperfection resonances during the acceleration from 500 MeV to 12 GeV in KEK proton synchrotron. Resonance strength is calculated by S. Hiramatsu and K. Muto<sup>(10)</sup> as shown in Fig. 2-5. They proposed to overcome them by means of  $\nu$ -jump and adiabatic passage.

In 1984 we will have polarized beam in Japan and US again.

There are several types of polarized ion sources. Among them the atomic beam type ion source was adopted for polarized beam at Argonne.<sup>(11)</sup> In this method a ground state  $^1S_{1/2}$  atomic beam is polarized by the Stern-Gerlach method. A schematic diagram of an atomic source is shown in Fig. 2-6. Atoms are generated by dissociating molecules in a low pressure discharge, and flow through nozzle and form a supersonic beam. The beam is polarized by passing through an inhomogeneous magnetic field, usually produced

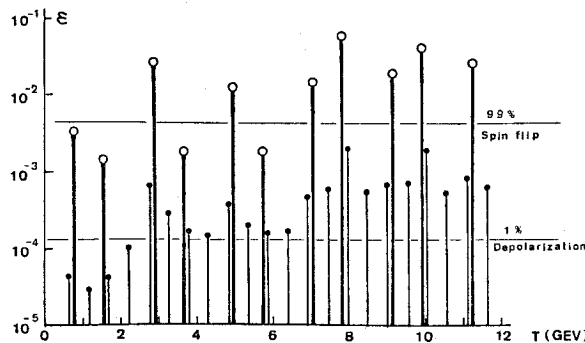


Fig. 2-5 Resonance strength in KEK PS calculated by Hiramatsu et al. Open circles are the strengths of intrinsic resonances and filled circles are the strengths of imperfection ones.



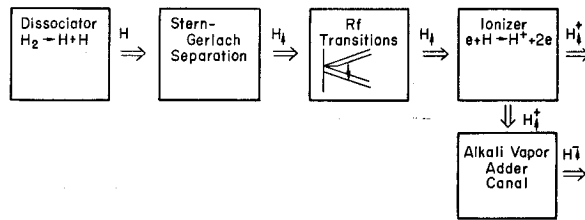


Fig. 2-6 A schematic diagram of an atomic source

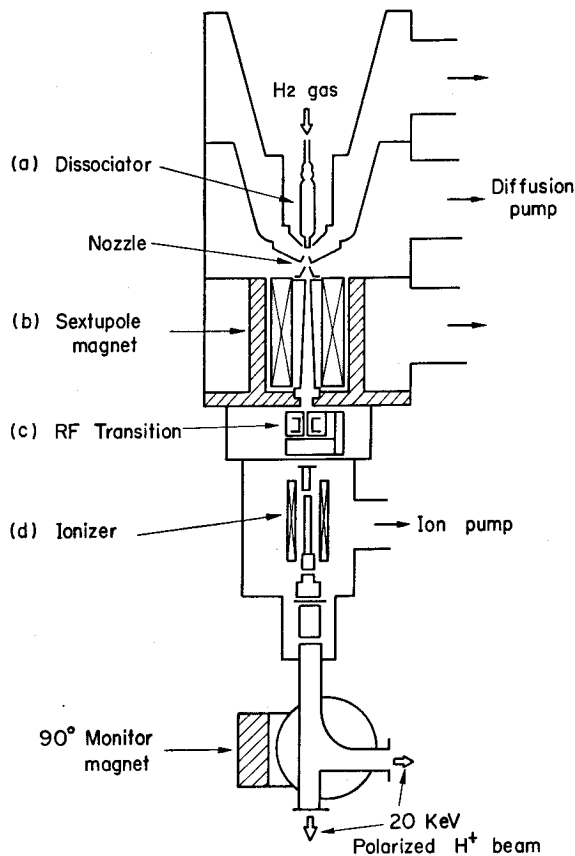


Fig. 2-7 Argonne polarized ion source

by a sextupole magnet. Rf transitions are induced between the hyperfine states of the atoms to enable different nuclear polarization states to be selected, and provide rapid spin reversal. The polarized atomic beam is then ionized. Positive ions are produced by electron bombardment. An adder canal can be used to convert them to negative ions. Schematic view of the Argonne polarized ion source is shown in Fig. 2-7. We can get the beam intensity of about  $50 \mu A$  by this method.

Recently a new method to polarize  $H^-$  ion utilizing a charge-exchange reaction between a fast proton beam and polarized Na atoms was proposed by Y. Mori et al. at

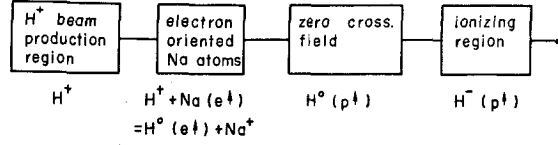


Fig. 2-8 The principle of polarized  $H^-$  ion source utilizing a charge-exchange reaction between a fast proton beam and polarized Na atoms.

KEK.<sup>12)</sup> The principle is shown in Fig. 2-8. Na atoms with polarized electrons are produced by optical pumping with intense cw dye laser tuned on the Na D1 line whose wavelength is 589.6 nm. From a preliminary experiment, they got already more than  $50 \mu A$ . This method will be applied to the polarized beam at KEK in near future.

### III. RECENT TOPICS ON POLARIZATION EXPERIMENT FOR THE SEARCH OF EXOTIC RESONANCES.

#### i) Nucleon-nucleon Scattering

There are several interesting topics on the nucleon-nucleon scattering using the polarized target and (or) the polarized beam. Before we will explain experimental results, we define the scattering amplitude. We can describe the scattering completely by the following 5 s-channel helicity amplitudes.

$$\left. \begin{aligned} \phi_1 &= \langle ++ | \phi | ++ \rangle \\ \phi_2 &= \langle -- | \phi | ++ \rangle \\ \phi_3 &= \langle +- | \phi | +- \rangle \\ \phi_4 &= \langle +- | \phi | -+ \rangle \\ \phi_5 &= \langle ++ | \phi | +- \rangle \end{aligned} \right\} \begin{array}{l} \text{net helicity non-flip} \\ \text{helicity double flip} \\ \text{helicity single flip} \end{array} \quad (3-1)$$

$\phi_1 \sim \phi_5$  can be written in t-channel exchange amplitudes.

$$\left. \begin{aligned} N_0 &= \frac{1}{2}(\phi_1 + \phi_2), \\ N_1 &= \phi_5 \\ N_2 &= \frac{1}{2}(\phi_4 - \phi_2) \\ U_0 &= A = \frac{1}{2}(\phi_1 - \phi_3) \\ U_2 &= \pi = \frac{1}{2}(\phi_4 + \phi_2), \end{aligned} \right\} \quad (3-2)$$

where  $N$  and  $U$  are natural and unnatural parity exchange amplitudes, respectively.  $U_0$  corresponds to  $A_1$  exchange and  $U_2$  corresponds to  $\pi$  exchange. The subscripts correspond to the total s-channel helicity.<sup>13)</sup>

The relations between observables and scattering amplitudes are as follows

$$\frac{d\sigma}{d\Omega} = \frac{1}{2} \{ |\phi_1|^2 + |\phi_2|^2 + |\phi_3|^2 + |\phi_4|^2 + 4|\phi_5|^2 \} \quad (3-3)$$

$$P = -\text{Im} \{ \phi_5^* (\phi_1 + \phi_2 + \phi_3 - \phi_4) \} \quad (3-4)$$

$$(1 - C_{NN}) = \frac{1}{2} \{ |\phi_1 - \phi_2|^2 + |\phi_3 + \phi_4|^2 \} \quad (3-5)$$

$$C_{LL} = \frac{1}{2} \{ -|\phi_1|^2 - |\phi_2|^2 + |\phi_3|^2 + |\phi_4|^2 \} \quad (3-6)$$

$$\Delta\sigma_L = \sigma^{tot}(\leftarrow\rightarrow) - \sigma^{tot}(\rightarrow\rightarrow) = -\frac{4\pi}{k} \text{Im}\{\phi_1(0) - \phi_3(0)\} \quad (3-7)$$

$$\Delta\sigma_T = \sigma^{tot}(\uparrow\downarrow) - \sigma^{tot}(\uparrow\uparrow) = -\frac{4\pi}{k} \text{Im}\phi_2(0) \quad (3-8)$$

where  $P$  is the polarization parameter.  $C_{NN}$  is a spin correlation parameter, in which the beam and the target are polarized with parallel and antiparallel spin directions perpendicular to the scattering plane.  $C_{LL}$  is also a spin correlation parameter, in which the beam and the target are polarized in the direction of the beam.  $\Delta\sigma_L$  means the difference between total cross section for antiparallel and parallel spin state in the longitudinal direction, while  $\Delta\sigma_T$  means that in the transverse direction.  $\phi(0)$  is a  $s$ -channel helicity amplitude at  $\theta_{cm} = 0$ .

$\Delta\sigma_L$  was measured in Argonne from 1.0 to 6.0 GeV/c with the longitudinally polarized incident protons and target protons. The experimental setup is shown in Fig. 3-1. They found unexpected structures in  $\Delta\sigma_L$ . The experimental results are shown in Fig. 3-2. There is a sharp peak near 1.2 GeV/c and a dip near 1.5 GeV/c. From Eq. 3-7

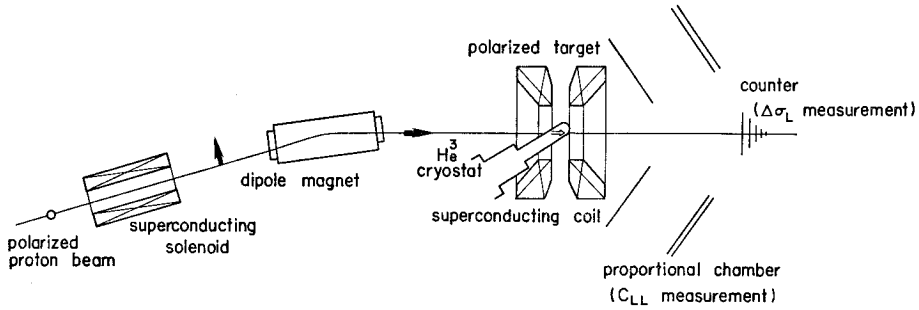


Fig. 3-1 Experimental setup for the measurement of  $\Delta\sigma_L$  at Argonne.

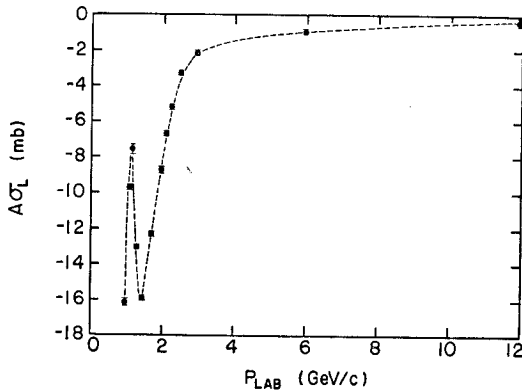


Fig. 3-2 Experimental results of total cross section difference  $\Delta\sigma_L$  at Argonne.

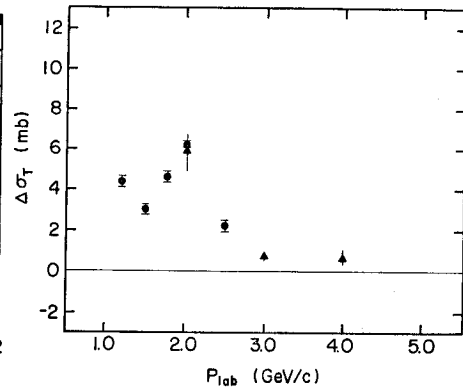


Fig. 3-3 Experimental results of  $\Delta\sigma_T$  at Argonne.

a structure in  $\phi_1(0)$  and  $\phi_3(0)$  should appear as a peak and dip in  $\Delta\sigma_L$  respectively. The results of  $\Delta\sigma_T$  measurements up to 4 GeV/c are also shown in Fig. 3-3. A peak at 2.0 GeV/c is clearly visible in  $\Delta\sigma_T$ .<sup>13)</sup>

Using the data on  $\Delta\sigma_L$ , Grein and Kroll calculated the real part of  $[\phi_1(0) - \phi_3(0)]$  by dispersion relations, and they found a resonance-like behavior in the Argand plot of  $[\phi_1(0) - \phi_3(0)]$  around the incident proton momenta of 1.5 GeV/c and 1.2 GeV/c.<sup>14)</sup>

Hoshizaki performed the phase shift analysis of p-p scattering ( $I=1$ ) up to 2.0 GeV/c using all the available data on  $pp$  scattering. His analysis gave strong indication of resonances in  $^1D_2$  and  $^3F_3$  states,<sup>15)</sup> as shown in Fig. 3-4.  $^1D_2$ -wave resonance has mass of  $\sim 2170$  MeV and the width of  $50\sim 100$  MeV with elasticity of  $\sim 0.1$ .  $^3F_3$ -wave

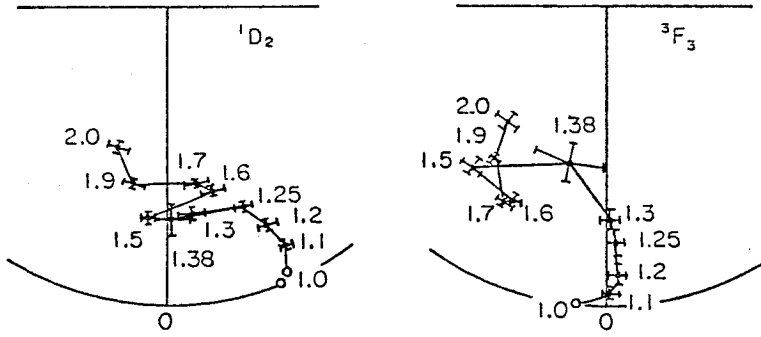


Fig. 3-4 Argand diagrams of  $^1D_2$  and  $^3F_3$  partial waves of  $pp$  scattering (points are in GeV/c)

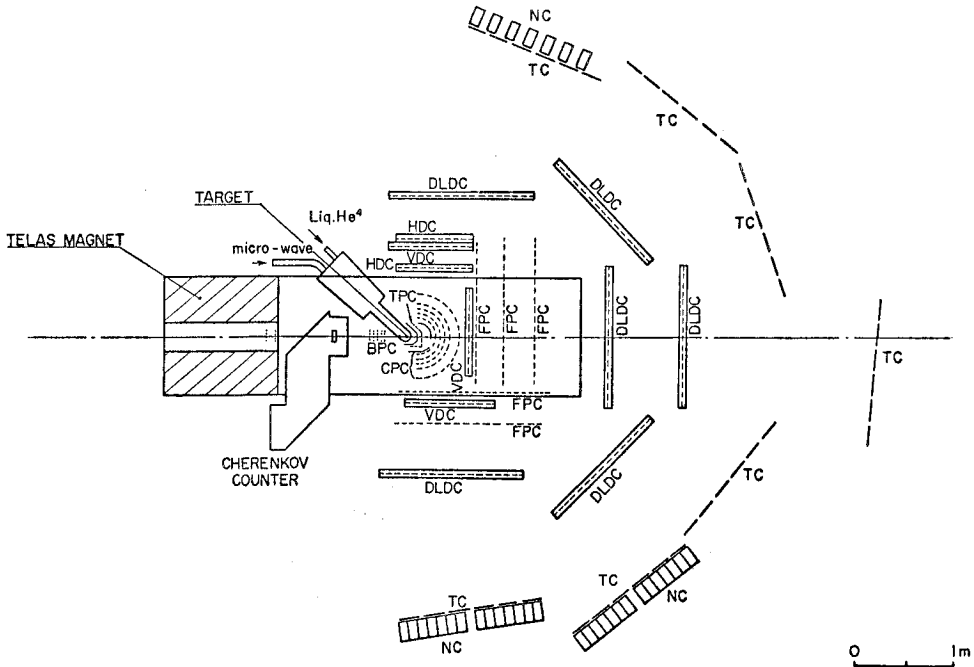


Fig. 3-5 TELAS spectrometer at KEK

resonance has mass of  $\sim 2220$  MeV, width of  $100\sim 150$  MeV and elasticity of  $\sim 0.2$ . These resonances correspond to the peak and the dip in  $\Delta\sigma_L$ . Recently Arndt extended and revised his energy dependent and energy independent phase-shift analysis up to  $1.5$  GeV/c and gave similar results as Hoshizaki's analysis.<sup>13)</sup>

On the other hand, Kamae *et al.* found an anomalous enhancement in the recoil proton polarization in the photodisintegration of the deuteron and suggested a possible existence of  $I=0$  resonances.<sup>16)</sup> Measurement of  $\Delta\sigma_L(I=0)$  at Argonne showed a structure around  $1.4$  GeV/c.<sup>13)</sup> Moreover Kleinschmidt *et al.* reported that  $I=0$  inelastic cross section showed a rapid increase around  $1.2$  GeV/c.<sup>17)</sup> Hoshizaki *et al.* suggested a possible resonance of  $I=0$  on the basis of  $pn$  phase shift.<sup>18)</sup>

In order to perform the detailed analysis of  $I=0$ , we measured the polarization parameter of the  $pn$  elastic scattering at  $1.3\sim 1.82$  GeV/c, using TELAS spectrometer system at KEK.<sup>19)</sup> A schematic view of the apparatus is shown in Fig. 3-5. It has a "C-type" magnet with a large gap (1 m), in which additional rectangular pole pieces were attached on the pole faces of the magnet in order to get polarizing magnetic field for the target. A horizontal dilution refrigerator was inserted at the center of the pole pieces. Deuterons in the propanediol were polarized up to 43 %. Several types of multi-wire proportional chambers, drift chambers with two-dimensional readout system using delay lines and counter hodoscopes were installed inside and outside of the magnetic field. The experimental results are shown in Fig. 3-6.<sup>20)</sup> There is no significant energy dependence in the angular distribution of polarization parameters below  $1.6$  GeV/c. The fact suggests that there is no spin triplet resonance in this energy region. The resonance should be spin singlet. It is consistent with the resonance like structure in the  ${}^1F_3$ -wave. Results of a phase shift analysis performed by Hashimoto and Hoshizaki using the

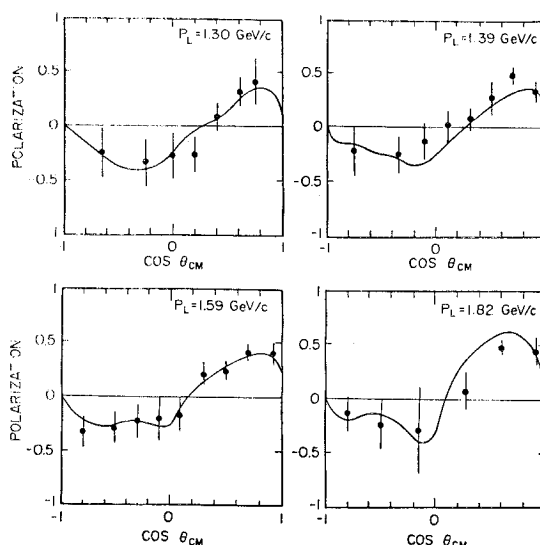


Fig. 3-6 Results of the polarization measurement of  $pn$  elastic scattering at KEK. Solid lines are the prediction of the phase shift analysis by Hashimoto and Hoshizaki.

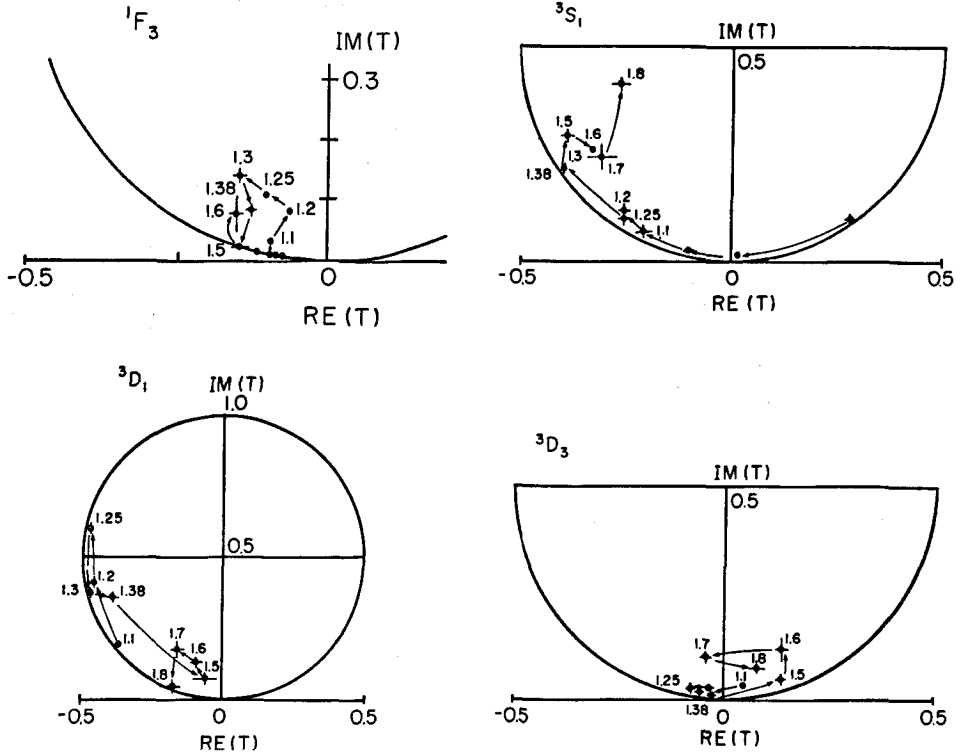


Fig. 3-7 Argand plots of  $pn$   $I=0$  partial waves,  $^1F_3$ ,  $^3S_1$ ,  $^3D_1$  and  $^3D_3$  by Hashimoto and Hoshizak.

polarization data are shown in Fig. 3-6.<sup>20)</sup> The Argand plots of  $^3S_1$ ,  $^3D_1$ ,  $^3D_3$  and  $^1F_3$  waves of their analysis are shown in Fig. 3-7. There are energy dependent structures in several states in the higher energy region. Especially  $^3D_1$  and  $^3D_3$  states are candidates for the  $I=0$  dibaryon resonances.

## ii) $Z^*$ Resonances and $K^+n$ Reactions

$K^+$ -nucleon systems would be exotic states, namely, four quarks and one strange antiquark, if  $K^+$ -nucleon resonances exist. Structures in  $K^+p$  and  $K^+d$  total cross sections suggest s-channel resonances in both  $I=1$  and  $I=0$  states. Search for an  $I=1$  state of  $K^+N$  interaction was made, studying  $K^+p$  systems from more than ten years ago. On the other hand, phase shift analysis of  $I=0$  system was performed by Giacomelli et al. (BGRT-group)<sup>21)</sup> and Martin.<sup>22)</sup> BGRT-group found three solutions (A, C and D solutions). In D-solution, the  $P_{01}$  wave has a resonance like behavior at the mass of 1.740 GeV, while in A and C solutions there is no significant evidence for the resonance. The energy dependent analysis of both  $I=0$  and  $I=1$  states made by Martin does not agree with the solutions of BGRT-group and has no clear conclusion on the resonance. These solutions give different predictions for polarization parameters of  $K^+n \rightarrow K^+n$ ,  $K^0p$  reactions.

At KEK we measured the polarization parameters of  $K^+n \rightarrow K^+n$ ,  $K^0p$  reactions at

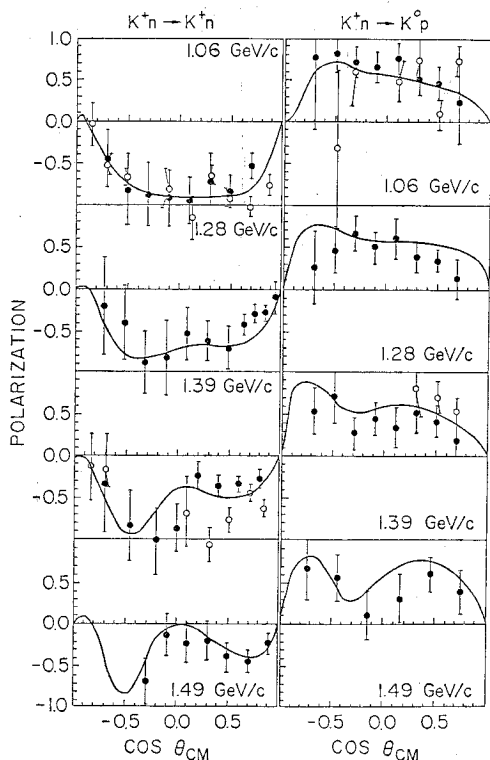


Fig. 3-8 Experimental results of polarization parameters for  $K^+n \rightarrow K^+n$ ,  $K^+p$  at KEK. Open circles are from Ref. 24. The solid lines show the prediction of the analysis by K. Nakajima *et al.*

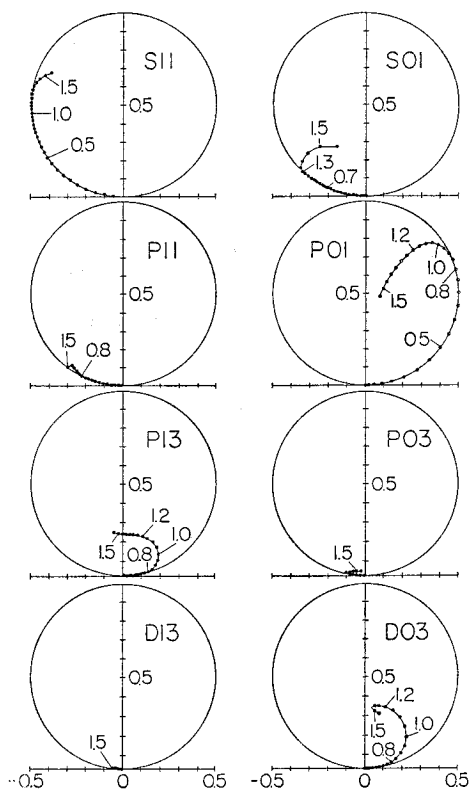
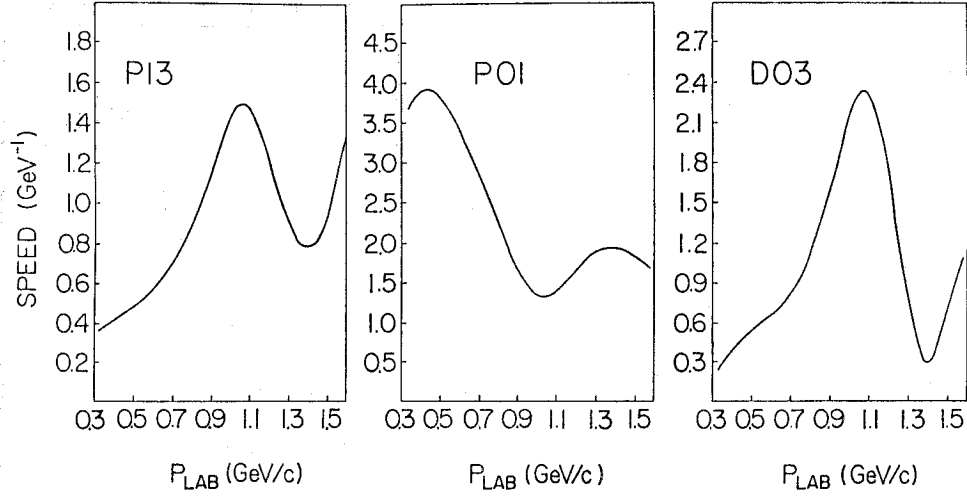


Fig. 3-9 Argand plots of  $KN$  partial waves.

the momenta of 1.06~1.49 GeV/c. The results are shown in Fig. 3-8.<sup>23)</sup> The  $K^+n$  elastic scattering has the negative polarization and charge exchange process are mostly positive. The results were compared with the predictions of the phase shift analyses of BGRT and Martin. None of the solutions of thier analyses show good agreement with the data. A new energy dependent partial wave analysis was made using the data including our new polarization results and the recent data of Robertson *et al.*<sup>24)</sup> Two solutions among several solutions depending on the different starting parameters have chi-square per freedom of about 1.4. One of the two solutions reproduce well the real to imaginary ratio of both  $I=0$  and  $I=1$  amplitudes at the forward angles than the other solution. In Fig. 3-8, the predicted polarizations of the solution are shown. The solution agrees well with the experimental results. In Fig. 3-9, Argand diagrams for the various partial waves are shown.  $P_{13}$ ,  $P_{01}$  and  $D_{03}$  waves show counter clock-wise circles as the function of the energy. The resonance parameters of these three waves can be given as follows, assuming the Breit-Wigner formula for the resonance amplitudes in addition to the smooth background amplitudes.

Fig. 3-10 Speed plot for  $P_{13}$ ,  $P_{01}$  and  $D_{03}$  waves.

	Mass	Width	Elasticity
$P_{13}$	1931	347	0.24
$P_{01}$	1778	662	0.56
$D_{03}$	1907	291	0.35

In order to check the resonance like behaviors, speed plots were performed for these three waves as shown in Fig. 3-10. The speed plot for the  $P_{13}$  wave shows a visible peak at 1 GeV/c. The  $P_{01}$  wave has a large peak at 0.4 GeV/c which deviates far from the resonance position. The  $D_{03}$  wave presents an evidence for a resonance, because the speed plot shows a clear peak at 1 GeV/c.

As shown in Fig. 3-11 the bump at 1.1 GeV/c in the  $I=0$  total cross section arises from the  $D_{03}$  wave and large structure at 0.75 GeV/c is almost due to the  $P_{01}$  wave.<sup>25)</sup>  $I=1$  total cross section and the contributions of various partial waves are also shown in Fig. 3-11. The contribution of  $P_{13}$ -wave for the bump in the  $I=1$  total cross section is obvious.

Resonance like behavior in the  $D_{03}$  wave was also pointed out by K. Hashimoto recently with his single energy phase-shift analysis including our polarization data.<sup>26)</sup>

As is shown in this section, dibaryon resonances and  $Z^*$  resonances were suggested by the experiments using the polarized target and/or the polarized beam. Further experiments for the search of dibaryons with polarized particles are going on in KEK, CERN-Saclay, SIN and Los Alamos. Especially the measurements on the polarization parameters of  $\pi^+d$  elastic scattering and several spin dependent parameters of  $pn$  scattering will give us important informations on the details of nucleon-nucleon resonances. About the  $K^+N$  system, a measurement of the polarization parameter of  $K^+d$  elastic scattering is now going on at KEK. It should be another check of the 4 quarks and 1 antiquark system.

We believe that other exotic resonances, as baryoniums (2 quarks-2 antiquarks) and strangeness dibaryons, can be confirmed by the measurements of spin dependent para-



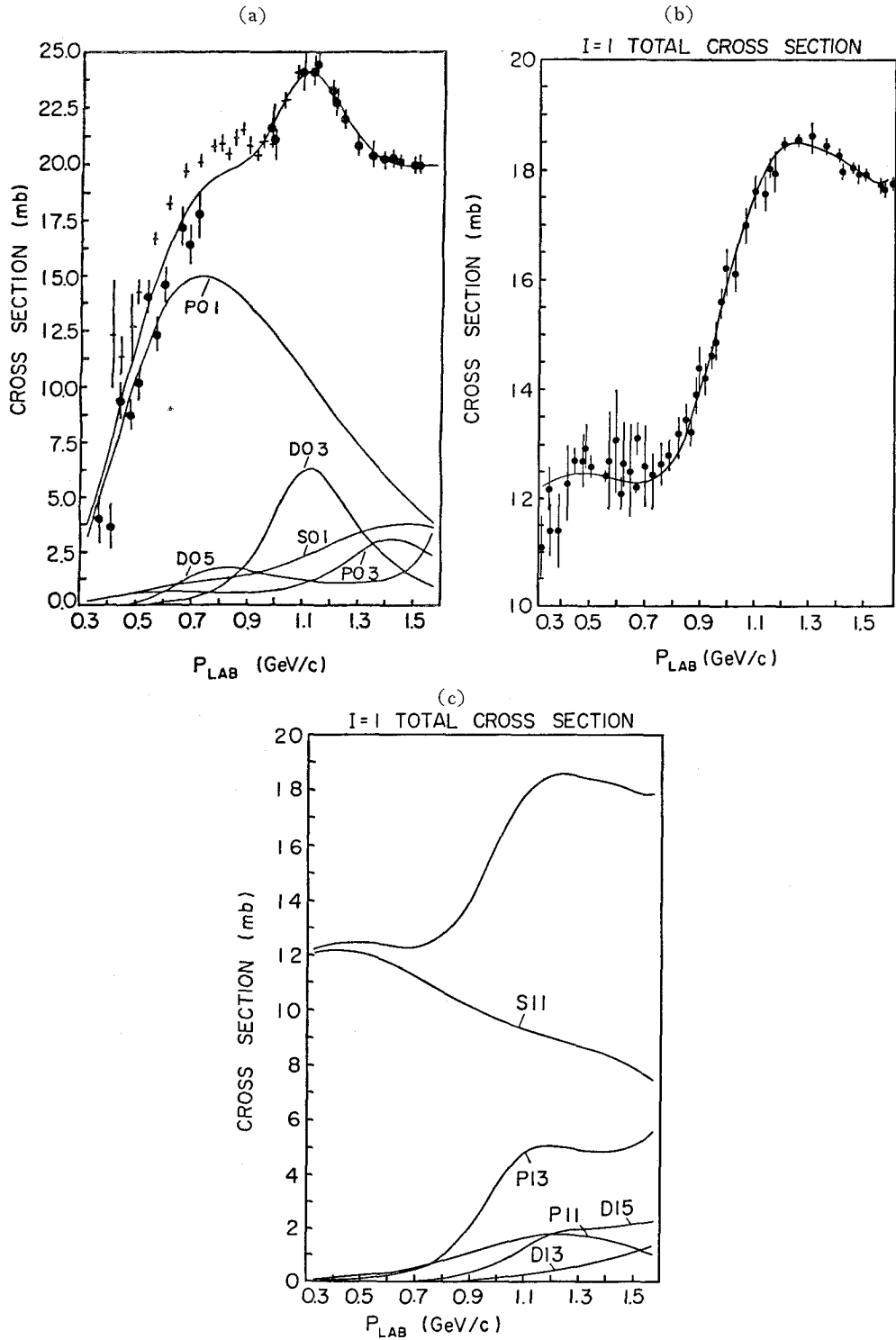


Fig. 3-11 Partial wave contributions to the total cross section for  
(a)  $I=0$  and (b), (c)  $I=1$  states of  $K^+N$ .<sup>25)</sup>

meters of the reactions.

I should like to express my sincere thanks to the members of "KN-group" with whom I made the experiments of  $Kn$  and  $pn$  experiments. I am also grateful to Drs. S. Hiramatsu, S. Isagawa, S. Ishimoto, Y. Mori and Prof. K. Morimoto for their co-operations and advices about the polarized target and the polarized beam.

## REFERENCES

- (1) A. Abragam, in *Proc. of Inter. Conf. on Pol. Targets and Ion Sources* (Saclay 1966) P. 28.
- (2) A.W. Overhauser, *Phys. Rev.*, **92**, 411 (1953).
- (3) A. Abragam, *Phys. Rev.*, **98**, 1729 (1955).  
A. Abragam and W.G. Proctor, *Compt. Rend.*, **246**, 2253 (1958).
- (4) A. Msaiké *et al.*, *Phys. Lett.*, **30A**, 63 (1969).
- (5) S. Isagawa *et al.*, *Nucl. Inst. Meth.*, **154**, 213 (1978).  
S. Ishimoto *et al.*, *Nucl. Inst. Meth.*, **171**, 269 (1980), and to be published.
- (6) T.O. Niinikoski and F. Udo, *Nucl. Inst. Meth.*, **134**, 216 (1976).
- (7) S. Hiramatsu *et al.*, *Jap. Jour. App. Phys.*, **19**, 161 (1980).
- (8) O. Hamada *et al.*, *Nucl. Inst. Meth.*, **189**, 561 (1981).
- (9) M. Froisart and R. Stora, *Nucl. Inst. Meth.*, **1**, 297 (1960).
- (10) S. Hiramatsu and K. Muto, *Proc. 1980 Int. Symp. on High Energy Physics with Pol. Beams and Pol. Targets* (Lausanne) P. 475.
- (11) H.F. Glavish, *Higher Energy Polarized Proton Beams*, AIP Conference Proc. No. 42. P. 47.
- (12) Y. Mori *et al.*, *Proc. 1980 Intern. Symp. on High Energy Physics with Pol. Beams and Pol. Targets* (Lausanne) P. 439.
- (13) A. Yokosawa, *Phys. Reports*, **64**, 50 (1980).
- (14) W. Grein and P. Kroll, *Nucl. Phys.*, **B137**, 173 (1978).
- (15) N. Hoshizaki, *Prog. Theor. Phys.*, **60**, 1796 (1978) ; **61**, 129 (1979).
- (16) T. Kamae *et al.*, *Phys. Rev. Lett.*, **38**, 471 (1977).
- (17) M. Kleinschmidt *et al.*, *Z. Physik*, **A298**, 253 (1980).
- (18) K. Hashimoto *et al.*, *Prog. Theor. Phys.*, **64**, 1678 (1980) ; **64**, 1693 (1980).
- (19) K. Nakajima *et al.*, *Nucl. Inst. Meth.*, **192**, 175 (1982).
- (20) M. Sakuda *et al.*, *Phys. Rev.* **25D**, 2004 (1982).
- (21) G. Giacomelli *et al.*, *Nucl. Phys.* **137**, 138 (1974).
- (22) B. Martin, *Nucl. Phys.*, **B94**, 413 (1975).
- (23) K. Nakajima *et al.*, *Phys. Lett.* **112B**, 75 (1982) ; **112B**, 80 (1982).
- (24) A.W. Robertson *et al.*, *Phys. Lett.*, **91B**, 465 (1980).  
S.J. Watts *et al.*, Rutherford Lab. RL-80-039 (1980).
- (25) K. Nakajima, Doctor Thesis (Tokyo Univ. 1981).
- (26) K. Hashimoto, *Prog. Theor. Phys.*, **66**, 2300 (1981).